

Control of Molecular Orientation in Electrostatically Stabilized Ferroelectric Liquid Crystals

D. Coleman, D. Mueller, N. A. Clark, J. E. MacLennan, R.-F. Shao, and S. Bardon

Department of Physics and Ferroelectric Liquid Crystal Materials Research Center, University of Colorado at Boulder, Boulder, Colorado 80309, USA

D. M. Walba

Department of Chemistry and Ferroelectric Liquid Crystal Materials Research Center, University of Colorado at Boulder, Boulder, Colorado 80309, USA

(Received 31 October 2001; revised manuscript received 10 October 2002; published 24 October 2003)

The continuously reorientable (*XY*-like) ferroelectric polarization density of a chiral smectic liquid crystal is shown experimentally to produce nearly complete screening of the applied electric field in an appropriate cell geometry. This screening, combined with the expulsion of polarization charge for large polarization materials, is shown to produce electrostatic control of the orientation of a uniform optic axis or polarization field.

DOI: 10.1103/PhysRevLett.91.175505

PACS numbers: 61.30.Gd, 61.30.Eb, 81.40.Tv

Chiral smectic *C* (SmC^*) liquid crystals are fluid ferroelectrics characterized by the structure shown in Fig. 1(a), a one dimensional (1D) stacking of 2D liquid layers of rod-shaped molecules having a mean long axis (optic axis) tilted through a fixed angle θ from the layer normal. Such a chiral phase is required by the lack of reflection symmetry to have a macroscopic ferroelectric polarization \mathbf{P} , locally normal to both the mean long axis \mathbf{n} and to the layer normal \mathbf{z} [1]. The intimate coupling of optic axis orientation to \mathbf{P} is unique among ferroelectric materials to SmC^* s and makes possible a variety of useful effects based on reorientation of the optic axis on the tilt cone in response to applied field [2–5]. Although the magnitude of \mathbf{P} is fixed, depending only on temperature, its azimuthal orientation in the x - y plane, $\phi(\mathbf{r})$, is unconstrained when there is no electric field applied [$\phi(\mathbf{r})$ is a Goldstone variable]. Then the SmC^* energy, independent of $\phi(\mathbf{r})$, depends only on its spatial derivatives, with contributions arising from molecular orientation curvature elasticity, surface interaction energy, and from the electrostatic self-interaction of the polarization charge density $\rho_P = -\nabla \cdot \mathbf{P}(\mathbf{r})$ [1].

In this Letter we verify that the *XY*-like orientational freedom of \mathbf{P} can lead to a particularly elegant mode of bulk ferroelectric electro-optic response. High polarization materials have an electro-optic response consistent with complete screening by polarization charge of the applied field in the liquid crystal (LC), exhibiting continuous orientation of uniform polarization and optic axis fields controlled solely by electrostatic interactions. We confirm key predictions of a recently proposed model of such behavior [6].

This model recognizes that the spatial variation of $\phi(\mathbf{r})$ in a SmC^* results in polarization charge $\rho_P(\mathbf{r})$ [Fig. 1(b)] which gives rise to nonzero electric field E_{LC} in the liquid crystal and an associated electrostatic energy, assuming that the LC is insulating and that ρ_P cannot be compensated by free charge. This energy contribution typically

increases as P^2 , eventually becoming dominant, in which limit splay of \mathbf{P} is expelled from the bulk SmC^* , rendering $\phi(\mathbf{r})$ uniform in the bulk [Fig. 1(c)] [7–16]. Nonuniform surface layers (polarization stabilized kinks [11]) of thickness $\xi_P = (\epsilon_{\text{LC}}K/P^2)^{1/2}$ may remain, where ϵ_{LC} is the bare LC dielectric constant (excluding effects of P) and K is the nematic-like orientational elasticity. However, the surfaces, which must apply a torque density $\tau \sim K/\xi_P$ to maintain these kinks, will be unable to do so at sufficiently large P , since eventually τ will exceed the available polar surface energy density. In this limit $\mathbf{P}(x)$ is predicted to become uniform from surface to surface giving good optical extinction (high-contrast) between crossed polarizers [6]. The dynamical equation governing the orientation of \mathbf{P} is then

$$\gamma \frac{\partial \phi}{\partial t} = -PE \sin \phi, \quad (1)$$

where γ is the viscosity for reorientation on the cone. Equation (1) can be rewritten as $J = \sigma E$, where $\sigma = (P^2 - P_E^2)/\gamma$ is the effective LC electrical conductivity associated with the reorientation of \mathbf{P} , and P_E is the component of \mathbf{P} along \mathbf{E} . With insulating layers on the cell surfaces [each of thickness t and dielectric constant ϵ , Fig. 1(d)] the electrostatic energy is nonzero, and is minimized by the orientation of \mathbf{P} for which $E_{\text{LC}} = 0$ [as required by Eq. (1) for quasistatic changes], i.e., for which the polarization charge density on the inside of the insulating layers, $P \cos \phi$, is equal in magnitude and opposite in sign to $\epsilon V/2t$, the free charge density on the outside of the insulating layer. Here V , the voltage applied to the cell, appears entirely across the insulating layer. This leads to an extremely simple relation between orientation on the cone and applied voltage [6],

$$\phi(V) = \cos^{-1}(\epsilon V/2tP), \quad (2)$$

which predicts analog electro-optic behavior with a voltage sensitivity that scales with insulating layer

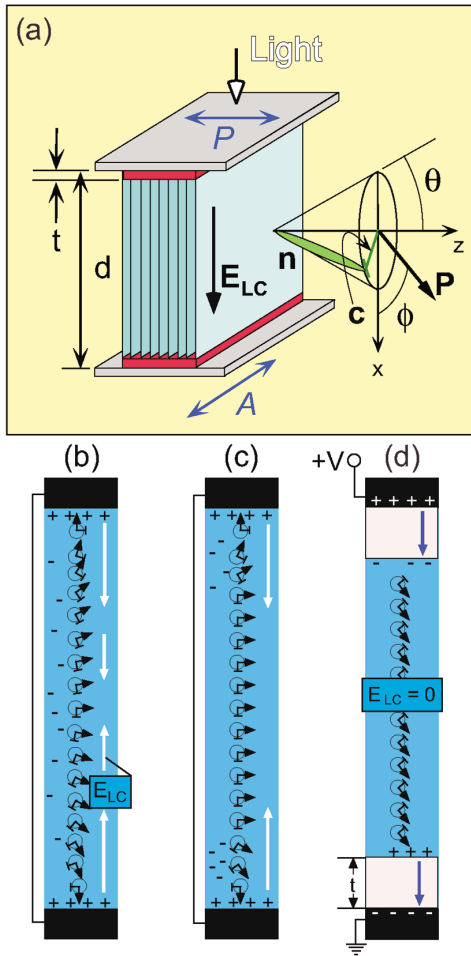


FIG. 1 (color online). (a) Bookshelf smectic liquid crystal cell geometry. The tilted chiral liquid crystal is a dielectric in a transparent ITO-glass capacitor, with the smectic layers more or less normal to the plates. Shown are the director \mathbf{n} , the tilt cone angle θ relative to the layer normal \mathbf{z} , the polarization \mathbf{P} , the \mathbf{c} director (the projection of \mathbf{n} onto the layer plane), the azimuthal orientation ϕ of $\mathbf{c}-\mathbf{P}$, and the cell normal \mathbf{x} . The cells have total thickness d , with alignment layers of thickness t on each surface. (b)–(d) Model structures of Sm-C^* SSFLC cells with \mathbf{c} indicated by \leftarrow and \mathbf{P} by \rightarrow . (b) Twisted structure resulting from strong polar surface anchoring. The resulting splay in the polarization causes a polarization charge density, and thus a nonzero electric field, within the cell. (c) Large \mathbf{P} excludes splay from the cell interior, reducing the electrostatic energy at the cost of elastic energy. (d) With insulating alignment layers present, polarization screening excludes the electric field from the LC and the applied voltage is dropped entirely across the alignment layers.

thickness, and counterintuitively, inversely with the magnitude of \mathbf{P} .

We report here experimental tests of four key predictions of this high- P regime model: (i) the spatial dependence of \mathbf{P} ; (ii) the $\phi(V)$ dependence; (iii) the dependence of the saturation voltage on the insulating layer thickness, t ; (iv) the independence of the saturation voltage on cell thickness, d . While features (ii)–(iv), and the bulk

orientation of $\mathbf{P}(x)$ can be probed using standard polarized transmission microscopy, studying $\mathbf{P}(x)$ requires distinct measurement of the surface and bulk orientations of \mathbf{n} , which we have carried out using the total internal reflection (TIR) evanescent wave method pioneered in our laboratory [13,17].

The experimental setup is presented in the inset to Fig. 2(a). An oblique He-Ne laser beam polarized in the plane of incidence passes through a high index hemisphere and into a glass slide (hemisphere and glass have $n = 1.802$ and are joined by index matching fluid), and illuminates the planar LC-glass interface at a fixed angle of incidence of 75° . The glass is coated with 327 \AA of indium tin oxide (ITO, $n = 1.917$) and a $\sim 500 \text{ \AA}$ thick polymer alignment layer. The light is totally reflected at the glass/ITO/polymer/LC interface, and an evanescent wave (probe beam) propagates along the interface in the polymer and the LC. The penetration depth into the LC is $\lambda_p \sim 1000 \text{ \AA}$. The depolarization ratio $R(\alpha)$ (the ratio of

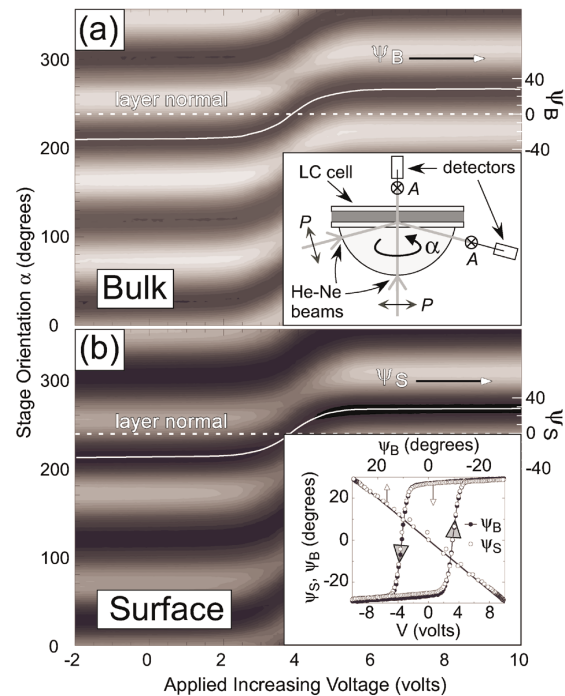


FIG. 2 (color online). (a) Contour plot of the transmitted intensity $T(\alpha, V)$ of 632 nm light through a bookshelf-aligned **W415** cell placed between crossed polarizers, as a function of increasing applied voltage and of azimuthal orientation. Right axis: Apparent bulk director orientation ψ_B relative to \mathbf{n} , determined from the minima of $T(\alpha)$. Inset: Setup for TIR study of the LC orientation near the glass surface via depolarization of the reflected He-Ne beam. The beam along the hemisphere axis probes the director field of the bulk LC. (b) Contour plot of the corresponding depolarized TIR intensity $R(\alpha, V)$. Right axis: Apparent surface director orientation ψ_S relative to \mathbf{n} , determined from the minima of $R(\alpha)$. Inset, hysteresis loop: Apparent bulk and surface director orientation dependence on applied voltage. Inset, line: ψ_S vs ψ_B . The cell was driven with a 20 Hz, 20 V_{pp} triangle wave.

the detected depolarized intensity to the incident intensity) is measured as a function of α , the angle between the layer normal and the plane of incidence. A second polarized He-Ne beam is normally incident on the cell, and measurement of its transmission $T(\alpha)$ through an analyzer oriented perpendicular to the polarizer enables characterization of the optic axis behavior in the bulk LC.

Studies were made of two high- P Sm- C^* materials in 1–3 μm thick, planar-aligned cells by using rubbed nylon films on one of the plates. The materials studied (the Walba compound **W415** [Iso $\xrightarrow{34.3^\circ\text{C}}$ Sm- A^* $\xrightarrow{24.1^\circ\text{C}}$ Sm- C^* $\xleftarrow{<0^\circ\text{C}}$ crystal; $P \approx 230 \text{ nC/cm}^2$] [18], and the three-component mixture of Fukuda and co-workers **T3** (Iso $\xrightarrow{69^\circ\text{C}}$ Sm- A^* $\xrightarrow{64^\circ\text{C}}$ Sm- C^* $\xrightarrow{43^\circ\text{C}}$ Sm- C_A^* ; $P \approx 100 \text{ nC/cm}^2$)[19]) were chosen to have P sufficiently large to ensure that $\xi_P < d$. The results of the **W415** experiments will be detailed here [20]. All experiments were performed at 19°C where for ac voltages at frequencies between $0.1 \leq f \leq 1.2 \text{ Hz}$, the cells exhibited an analog electro-optic response as predicted by Eq. (2).

In Fig. 2, we present contour plots of $R(\alpha, V)$ and $T(\alpha, V)$ as a function of stage orientation and applied voltage obtained by applying a 20 V, 20 Hz triangle wave to the cells and rotating the stage stepwise through 360° . The four minima in $R(\alpha)$ as the stage is rotated through 360° indicate the orientations where the projection of the average optic axis in the region probed by the reflected beam onto the surface plane is either parallel or perpendicular to the plane of incidence. The polarizer for the normally incident transmitted beam is aligned parallel to this plane of incidence so that we are able to compare directly the orientation of the optic axis of the bulk of the cell to that within λ_P of the ITO surface. The trajectories of the minima of $T(\alpha)$ [$R(\alpha)$] in the main plots of Fig. 2 show the field dependence of ψ_B (ψ_S), the orientation of the bulk (surface) optic axis projection into the surface plane relative to the layer normal in the increasing part of the triangle cycle. ψ_B and ψ_S are similar and the plot of ψ_S vs ψ_B in the inset of Fig. 2(b) verifies this, the data lying close to the line $\psi_S = \psi_B$. The complete triangle driven cycle exhibits hysteresis, a result of the orientational viscosity associated with the Goldstone mode and calculable from Eq. (1). As expected, the polarization stiffening maintains $\psi_S \approx \psi_B$ throughout this cycle. Positive voltages move the optic axes in the positive ψ direction such that the positive voltage saturation position has the bulk director lying along the rubbing direction due to the SEC as noted above [20]. In this limit, the surface optic axis also lies along the rubbing direction so that the director is uniform and undistorted, from the bulk all the way down to the surface. As the voltage decreases, the bulk optic axis rotates smoothly according to Eq. (2), until at large negative voltage the bulk director is oriented at -28° , on the other side of the tilt cone. The surface optic axis, however, does not rotate this far, saturating at -26° . The small deviation

from $\psi_B = \psi_S$ at negative V is due to either a uniform $\sim 50 \text{ \AA}$ thick layer of Sm- C^* adsorbed on the surface and oriented with its optic axis along the rubbing direction, or to strong polar pinning of the director at the surface (director along the rubbing direction) coupled with a rapid elastic relaxation to the bulk orientation over a distance $\xi \sim 80 \text{ \AA}$. In either case, with the exception of a thin surface layer, the entire $2 \mu\text{m}$ thick slab of liquid crystal is responding as a uniform block. For homogeneous motion on the cone, when $\psi = 0$ (the optic axis projection is along \mathbf{z}), $\phi = +90^\circ$ (or -90°) and the optic axis is tilted down (or up) by θ from the plane of the cell. In this case the minima in $R(\alpha)$ when \mathbf{z} is normal to the TIR plane of incidence are no longer zero and disappear for $\theta > 24^\circ$ [21]. In our experiments the depolarization at these sample orientations is vanishingly small, indicating that the evanescent beam samples a conglomerate of $\phi = +90^\circ$ and $\phi = -90^\circ$ domains.

We performed a systematic study of the dependence of the saturation voltage V_{sat} on alignment layer thickness [22]. By varying the spin coating speed, we produced nylon alignment layers with t in the range $200 \text{ \AA} < t < 1300 \text{ \AA}$ and a dielectric constant of $\epsilon_{\text{IL}} = 4.1 \pm 0.2$ as measured in a $6.4 \mu\text{m}$ thick film [23]. When assembled as sandwich cells, these substrates gave total insulator thicknesses $400 \text{ \AA} < 2t < 2600 \text{ \AA}$. Figure 3(a) shows the dependence of the saturation voltage in **W415** on $2t$. The data are fitted well by a straight line as predicted by the theory, but with a slope of $3.61 \pm 0.05 \text{ mV/\AA}$, which is 1.7 ± 0.1 times lower than the predicted value of $2P/\epsilon_{\text{IL}}$ calculated taking $P = 228 \pm 12 \text{ nC/cm}^2$. As noted above, ϵ_{IL} was not measured in the LC sandwich cells. Absorption of ionic impurities from the liquid crystal into the alignment layer would likely increase ϵ_{IL} and thus decrease the observed V_{sat} . Furthermore, these cells had a chevron layer structure as evidenced by zigzag defects. Because the chevron forces some component of \mathbf{P} parallel to the plane of the cell, V_{sat} is decreased by the reduction in the effective polarization of the LC.

Finally, we measured the dependence of the saturation voltage dependence on cell thickness. We prepared cells with identical nylon alignment layers of thickness $t = 250 \text{ \AA}$. The cells were then assembled using different spacers with the resulting cell thickness in the range $1.9 \mu\text{m} \leq d \leq 4.4 \mu\text{m}$, measured by a visible light spectrometer. All of these cells had the analog, hysteresis-free electro-optic response. The measured saturation voltages are plotted in Fig. 3(b). Despite differences of more than a factor of 2 in cell thickness, the optical response of all of the cells saturates at approximately the same voltage, as expected for a liquid crystal in which the polarization expels electric field.

In summary, we have demonstrated a unique new property of tilted chiral smectic liquid crystals. In contrast to most previous liquid crystal observations in which the anchoring of the molecules at a solid surface governs

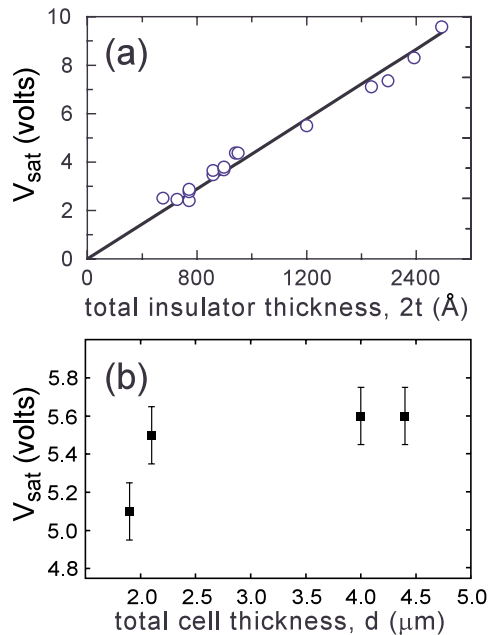


FIG. 3 (color online). (a) V_{sat} measured as a function of total alignment layer thickness. The solid line is the best fit to the data. (b) V_{sat} measured as a function of total cell thickness.

their behavior, the defining character in these high polarization materials is the self-interaction stiffening of the polarization field and the resulting screening of applied fields. Sufficiently large \mathbf{P} can overcome the surface anchoring, freeing the polarization to expel electric field from the LC. In this limit, the director dynamics are governed by the electrical properties of the cell rather than the usually dominant surface interactions, and the optical and electrical properties are partially decoupled: the thickness of the alignment layers can be tuned to adjust V_{sat} and the overall cell thickness can be tuned to adjust the optical thickness of the device.

This work was supported by NSF MRSEC Grant No. DMR 98-09555, DARPA Contract No. BOU431587, NASA Grant No. NAG3-1846, and NSF Grant No. DMR-96-14061.

-
- [1] R. B. Meyer, L. Liebert, L. Strzelecki, and P. Keller, *J. Phys. (Paris), Lett.* **36**, L69 (1975).
 - [2] M. A. Handschy, N. A. Clark, and S. T. Lagerwall, *Phys. Rev. Lett.* **51**, 471 (1983).
 - [3] N. A. Clark and S. T. Lagerwall, *Ferroelectrics* **59**, 25 (1984).
 - [4] M. A. Handschy and N. A. Clark, *Ferroelectrics* **59**, 69 (1984).
 - [5] J. S. Patel, *Appl. Phys. Lett.* **60**, 280 (1992).
 - [6] N. A. Clark, D. Coleman, and J. E. Maclellan, *Liq. Cryst.* **27**, 985 (2000).
 - [7] J. F. Palierne, *Phys. Rev. Lett.* **56**, 1160 (1986).
 - [8] K. Okano, *Jpn. J. Appl. Phys.* **25**, L846 (1986).
 - [9] I. Dahl, *Ferroelectrics* **84**, 327 (1988).

- [10] M. Nakagawa and T. Akahane, *J. Phys. Soc. Jpn.* **55**, 1516 (1986).
- [11] Z. Zhuang, J. E. Maclellan, and N. A. Clark, *Proc. SPIE Int. Soc. Opt. Eng.* **1080**, 110 (1989).
- [12] Z. Zhuang, Ph.D. thesis, University of Colorado, 1991 (Diss. Abst. No. AAG9220462).
- [13] Z. Zhuang, N. A. Clark, and M. R. Meadows, *Phys. Rev. A* **45**, R6981 (1992).
- [14] M.-H. Lu, K. Crandall, and C. Rosenblatt, *Phys. Rev. Lett.* **68**, 3575 (1992).
- [15] N. A. Clark, T. P. Rieker, and J. E. Maclellan, *Ferroelectrics* **85**, 79 (1988).
- [16] M. Guena, M. Le Gall, and L. Dupont, *Ferroelectrics* **213**, 45 (1998).
- [17] J. Z. Xue and N. A. Clark, *Phys. Rev. Lett.* **64**, 307 (1990).
- [18] **W415** is a nitroalkoxy-based room temperature Sm-C* [compound **3** in F. Stevens, D. J. Dyer, D. M. Walba, R. Shao, and N. A. Clark, *Liq. Cryst.* **22**, 531 (1997)].
- [19] T3 is a mixture of homologs of the antiferroelectric Sm-C_A* material **MHPOBC** [see A. Fukuda, in *Proceedings of the 15th International Display Research Conference of the Society for Information Display: Asia Display 1995* (Institute of Television Engineers of Japan, Tokyo, Japan, 1995), p. 61; S. Inui *et al.*, *J. Mater. Chem.* **6**, 671 (1996); S. S. Seomun *et al.*, *Jpn. J. Appl. Phys.* **37**, L691 (1998); A. Fukuda *et al.*, *J. Mater. Chem.* **4**, 997 (1994)].
- [20] In **W415**, the Sm-A* layer normal forms at the Iso-Sm-A* transition at an angle $\psi \approx 24^\circ$ from the rubbing direction due to the surface electroclinic effect (SEC). In order to obtain uniform alignment of the liquid crystal, it is necessary either to cross rub the two alignment layers at an angle of 48° so that the SEC tilts at each substrate effectively cancel, resulting in a uniform layer normal orientation throughout the cell, or to rub only one substrate. Cells made with either alignment technique have quantitatively identical electro-optic responses except for a small dc offset in the cells with one surface rubbed, due to the polar asymmetry of those cells from top to bottom [see R.-F. Shao, J. E. Maclellan, N. A. Clark, D. J. Dyer, and D. M. Walba, *Liq. Cryst.* **28**, 117 (2001)]. The one surface rubbing technique was used for the TIR cells and the cross-rubbing technique was used for the V_{sat} experiments.
- [21] J. Z. Xue, N. A. Clark, and M. R. Meadows, *Appl. Phys. Lett.* **53**, 2397 (1988).
- [22] The Tokyo group found independently that insulating layers promote a high-contrast, analog response (see Y. Takanishi, A. D. L. Chandani, Y. Cui, S. Seomun, K. Ishikawa, H. Takezoe, and A. Fukuda, in *Proceedings of the 17th International Liquid Crystal Conference, Strasbourg, 1998* (Centre National de la Recherche Scientifique, Université Louis-Pasteur de Strasbourg, Strasbourg, France, 1998), Poster P1-57; A. D. L. Chandani, Y. Cui, S. S. Seomun, Y. Takanishi, K. Ishikawa, H. Takezoe, and A. Fukuda, *Liq. Cryst.* **26**, 167 (1999).
- [23] ϵ_{IL} could not be measured in the actual 200–600 Å thick insulating layers due to difficulties arising from the dielectric loss in these thin films.